Journal for ImmunoTherapy of Cancer

Tumor CEMIP drives immune evasion of colorectal cancer via MHC-I internalization and degradation

Biying Zhang,[1,2] Jiao Li,[1,2] Qingling Hua,[1,2] Haihong Wang,[1] Guojie Xu,[1] Jiayuan Chen,[1] Ying Zhu,[1] Ruiqi Li,[1] Qing Liang,[1] Lanqing Wang,[1] Min Jin,[1] Jing Tang,[1] Zhenyu Lin,[1] Lei Zhao,[1] Dejun Zhang,[1] Dandan Yu,[1] Jinghua Ren,[1,2] Tao Zhang [1,2]

To cite: Zhang B, Li J, Hua Q, *et al*. Tumor CEMIP drives immune evasion of colorectal cancer via MHC-I internalization and degradation. *Journal for ImmunoTherapy of Cancer* 2023;**11**:e005592. doi:10.1136/jitc-2022-005592

► Additional supplemental material is published online only. To view, please visit the journal online (http://dx.doi.org/10.1136/jitc-2022-005592).

BZ, JL and QH contributed equally.

Accepted 15 December 2022

[1]Cancer Center, Union Hospital, Tongji Medical College, Huazhong University of Science and Technology, Wuhan, China
[2]Institute of Radiation Oncology, Union Hospital, Tongji Medical College, Huazhong University of Science and Technology, Wuhan, China

Correspondence to
Professor Tao Zhang;
taozhangxh@hust.edu.cn

Dr Jinghua Ren;
jhrenmed@hust.edu.cn

Dandan Yu;
yudandan@hust.edu.cn

ABSTRACT

Background Loss of major histocompatibility complex class I (MHC-I) in tumor cells limits the use of immune checkpoint blockade (ICB) in colorectal cancer. Nevertheless, the regulatory mechanism of MHC-I downregulation in tumor cells has not been fully elucidated. Overexpression of CEMIP in tumor tissues is associated with a poor prognosis in colorectal cancer. Here, in this research, we aim to address the role of CEMIP in mediating MHC-I expression in tumor cells and investigate the underlying regulatory mechanisms.

Method Protein levels were analyzed by western blotting. Flow cytometry analysis was used to examine immune cells. Protein–protein interactions were investigated by co-immunoprecipitation and proximity ligation assays. The intracellular trafficking of MHC-I was revealed by an immunofluorescent technique. In addition, the effect of CEMIP on tumor growth and the antitumor efficacy of targeting CEMIP in combination with ICB therapy were evaluated in murine models of colorectal cancer.

Results We reported that CEMIP specifically downregulated the expression of MHC-I on the surface of murine and human colon cancer cells, hindering the cytotoxicity of $CD8^+$ T cells. We also demonstrated that CEMIP restricted $CD8^+$ T-cell antitumor activities both in vitro and in vivo due to impaired MHC-I-mediated antigen presentation. Correspondingly, the combination of CEMIP inhibition and ICB impeded tumor growth and enhanced therapeutic efficacy. Mechanistically, CEMIP acted as an adaptor for the interaction betweenMHC-I and clathrin, which drove MHC-I internalization via clathrin-dependent endocytosis. Furthermore, CEMIP anchored internalized MHC-I to lysosomes for degradation, disrupting the recycling of MHC-I to the cell surface.

Conclusion Overall, our study unveils a novel regulatory mechanism of MHC-I on tumor cell surfaces by CEMIP-mediated internalization and degradation. Furthermore, targeting CEMIP provides an effective strategy for colorectal cancer immunotherapy.

WHAT IS ALREADY KNOWN ON THIS TOPIC?

⇒ Overexpression of CEMIP in tumor tissues is associated with a poor prognosis in colorectal cancer. Nevertheless, recent studies have mainly focused on the effect of CEMIP on cell invasion and migration while largely ignoring its immune-modulation function.

WHAT THIS STUDY ADDS?

⇒ CEMIP drives major histocompatibility complex class I (MHC-I) internalization via clathrin-mediated endocytosis and subsequently anchors MHC-I to lysosomes for degradation, resulting in the reduction of MHC-I levels on the cell surface.

HOW THIS STUDY MIGHT AFFECT RESEARCH, PRACTICE OR POLICY?

⇒ These findings highlight that CEMIP is a specific MHC-I negative regulator that hinders the cytotoxicity of $CD8^+$ T cells. Targeting CEMIP may synergize with immune checkpoint blockade for colorectal cancer immunotherapy.

BACKGROUND

Immune checkpoint blockade (ICB) therapy has been shown to induce remarkable responses in several cancer types, including melanoma, non-small cell lung cancer, and renal cell carcinoma.[1 2] However, due to primary or acquired resistance to ICB, most patients (~80%) fail to respond to checkpoint monotherapy.[3]$CD8^+$ T-cell dysfunction is the most straightforward mechanism of resistance to ICB.[4] Recently,numerous studies have placed the antigen presentation center stage in $CD8^+$ T cell-mediated immunosurveillance.[5–7] Several tumors impair antigen processing and peptide presentation to evade immune eradication.[8–11] Major histocompatibility complex class I (MHC-I), the key component in antigen presentation, presents peptide epitopes on the tumor cell surface for recognition by $CD8^+$ T cells and induces $CD8^+$ T-cell activation with the secretion of perforin, granzyme, and interferon to kill tumor cells.[12] MHC-I deficiency or downregulation on the tumor cell surface leads to insufficient antigen presentation and impedes

$CD8^+$ T-cell antitumor activity.[13] Upregulation of surface MHC-I expression is a promising strategy to improve ICB therapy for cancer.

To evade immune surveillance, tumor cells have developed various mechanisms to reduce the expression of MHC-I or other components of antigen presentation. Previous studies have mainly focused on MHC-I alterations at the genetic and transcriptomic levels, largely ignoring their intracellular trafficking.[14] A recent series of studies have shown that tumor cells can also exploit MHC-I trafficking and degradation to evade the immune response.[15–17] Similar to other cell surface receptors, MHC-I molecules are first internalized into the cytoplasm from the cell surface.[18] The internalized MHC-I molecules arrive at early sorting endosomes in a short time,[19] after which they are sorted into late endosomes and lysosomes for degradation or routed to the cell surface for recycling.[18] Internalization is a constitutive and important event for signal transduction of all plasma membrane components.[20] The abnormal internalization or degradation of MHC-I leads to reduced cell membrane abundance and consequent curtailment of $CD8^+$ T-cell antitumor activity.

Colorectal cancer (CRC) is the second leading cause of cancer-related death worldwide.[21] ICB has shown promise in treating patients with CRC, but the benefit has thus far been restricted to 15% of patients with CRC with microsatellite instability-high (MSI-H) or mismatch repair deficiency (dMMR).[22] The vast majority of patients with CRC do not respond to current immunotherapy. The genetic mutations in the antigen-presentation are a defined mechanism for immunotherapy resistance.[23] However, colon cancer is heavily immunoedited and harbors many mutations that are not present on antigen-presentation MHC. Genetic mutations in antigen-presentation, such as B2M, human leukocyte antigen (HLA)-A, HLA-B and HLA-C were low in patients with CRC.[24] Thus, an in-depth understanding of the intrinsic resistance mechanisms may contribute to the development of effective therapeutic strategies for these patients with CRC. We previously identified that CEMIP, an oncogene, was significantly higher in CRC tissue than in normal colonic mucosa and was associated with invasion depth, tumor, node, metastases stage, and poor clinical prognosis. Furthermore, it was reported that CEMIP was a direct and functional target of miR-216a and promoted tumor metastasis in CRC via microtubule destabilization regulated by a PP2A/stathmin pathway.[25] Here, we demonstrate that CEMIP could drive the internalization of MHC-I from the cell surface via clathrin-dependent endocytosis and then promote its degradation in the lysosome, by which CEMIP decreases the expression of MHC-I on the tumor cell surface and diminishes the cytotoxicity of $CD8^+$ T cells. Reciprocally, CEMIP inhibition could sensitize patients with CRC to ICB therapy.

METHODS

Animal experiments

OT-I transgenic mice, C57BL/6, and Balb/c mice (6–7 weeks old) were supplied by Vital River Laboratory (Beijing, China). CEMIP knockdown ($CEMIP^{KD}$), overexpression ($CEMIP^{OE}$), and scramble MC38 (3×10^5) or CT26 (5×10^5) cells were subcutaneously injected into the right flanks of these mice. Mice were monitored for tumor growth every 2 days afterward. Tumor size was calculated using the formula ($width^2\times length)/2$. For chlorpromazine (MedChemExpress, USA) and chloroquine (MedChemExpress, USA) treatment, mice respectively received intraperitoneal injections of chlorpromazine (10 mg/kg), chloroquine (60 mg/kg), or phosphate-buffered saline (PBS) one time per day for the duration of the experiment. For ICB experiments, mice were intraperitoneally injected with anti-mouse programmed cell death protein-1 (PD-1) antibody (200 µg/per mouse) and anti-mouse cytotoxic T-lymphocytes-associated protein 4 (CTLA-4) antibody (100 µg/per mouse) or IgG1 isotype monoclonal antibodies on day 3 after tumor cell inoculation and then every 3 days for the duration of the experiment.

OT-I T-cell isolation and co-culture with tumor cells

Splenic OT-I T cells were magnetically isolated by a MojoSort Mouse CD8+ T Cell Isolation Kit according to the manufacturer's protocol. Isolated OT-I T cells were first labeled with 10 µM carboxyfluorescein diacetate succinimide ester(BioLegend, USA) and then co-cultured with ovalbumin (OVA^+) tumor cells in Roswell Park Memorial Institute-1640 medium supplemented with 10% fetal bovine serum, 10 ng/ml interleukin (IL)-2 (BioLegend, USA) and 27.5 µM 2-mercaptoethanol. After 72 hours, the proliferation of $CD8^+$ T cells and secretion of interferon (IFN)-γ and granzyme B (GZMB) by $CD8^+$ T cells were analyzed using flow cytometry.

Flow cytometry analysis

For cell surface MHC-I analysis, cells were stained with fluorescent conjugated anti-MHC-I antibodies for human cell lines, APC conjugated anti-H-$2K^d$ antibody for CT26, Alexa Fluor 647 conjugated anti-H-$2K^b$ antibody for MC38 for 30 min on ice. Cells were then washed twice with RPMI 1640 and suspended in PBS to perform analysis. For tumor tissue flow cytometry analysis, tissues were minced and digested in RPMI 1640 containing 1 mg/mL collagenase V, 0.5 mg/mL hyaluronidase, and 100 µg/mL DNase I for 1 hour at 37°C. After red blood cell lysis, cells were blocked with anti-mouse CD16/CD32 (TruStain FcX, clone 93, BioLegend) and stained with a Zombie NIR Fixable Viability Kit (BioLegend). Cells were then incubated with the indicated fluorescent conjugated antibodies against the following mouse antigens: PerCP-Cy5.5-CD45, FITC-CD3, BV510-CD8, PE-CD4, PE-NK1.1, APC-FOXP3, BV421-IFNγ, and PE/Dazzle 594-GZMB (online supplemental table 2). Then, the cells were fixed in 4% paraformaldehyde and suspended in PBS.

Cells were analyzed on BD FACSCELEASTA, and all flow cytometry analysis (FACS) data were analyzed by FlowJo software (TreeStar, Ashland, USA).

Statistical analysis

Statistical analysis was performed using GraphPad Prism V.8 software (GraphPad Software). All the data are presented as the mean±SEM of at least three independent experiments. The statistics were analyzed by the SPSS V.17.0 statistical software package (SPSS, Illinois, USA). Data were evaluated by one-way analysis of variance with Bonferroni's multiple comparisons test for three or more groups and the unpaired two-tailed Student's t-test for two groups. Survival analysis was estimated by Kaplan-Meier methods. The log-rank test was used to calculate significant differences. P value<0.05 was considered to be statistically significant.

Additional methods can be found in the online supplementary methods.

RESULTS

CEMIP drives tumor growth and inhibits the antitumor activity of CD8$^+$ T cells

To evaluate the effects of CEMIP on tumor growth, we established CEMIP-overexpressing (CEMIP^{OE}) cells in two murine colon cancer cell lines (MC38 and CT26) using lentivirus infection. Interestingly, CEMIP^{OE} cells proliferated similarly to control cells in vitro (online supplemental figure 1A). In contrast, when CEMIP^{OE} cells were inoculated into syngeneic mouse hosts, mice bearing CEMIP-overexpressing tumor cells, including CEMIP^{OE} MC38 and CEMIP^{OE} CT26, exhibited faster tumor growth and shorter survival time than vector-control mice (figure 1A–D and online supplemental figure 1B,C). Consistently, faster tumor growth in CEMIP^{OE} MC38-bearing mice was confirmed in the orthotopically transplanted model in which tumor cells were implanted in the subserosa layer of the cecum (online supplemental figure 1D). Moreover, our previous study indicated that CEMIP has no effect on tumor cell proliferation in an orthotopic mouse model in NOD/SCID mice.[26] Together, these results imply that CEMIP-mediated tumor proliferation is dependent on the immune system.

To explore the main microenvironment elements involved in CEMIP-mediated tumor proliferation, we next analyzed the immune cell subsets of tumor tissues by FACS (online supplemental figure 1E). FACS showed that the number of tumor-infiltrating CD8$^+$ T cells in CEMIP^{OE} tumors significantly decreased compared with the control tumors (figure 1E,F). Immunofluorescence staining also confirmed that CEMIP caused an overall decrease in the tumor infiltration of CD8$^+$ T cells (online supplemental figure 1F). Moreover, the percentages of IFN-γ$^+$ CD8$^+$ T cells and GZMB$^+$ CD8$^+$ T cells were significantly reduced in CEMIP^{OE} tumors (figure 1E,F). We also found that the frequency of intratumoral Ki67-expressing CD8$^+$ T cells was lower in CEMIP^{OE} tumors than the control tumors (figure 1G and online supplemental figure 1G). In contrast, the percentages of CD3$^+$ T cells, CD4$^+$ T cells, CD4$^+$ Foxp3$^+$ regulatory T cells, and natural killer (NK) cells were not altered with CEMIP expression changes. Meanwhile, there was no difference in the percentages of CD4$^+$ T cells, CD8$^+$ T cells, and NK cells in the spleens between the two groups of mice (online supplemental figure 2A,B). Consistent with our findings in mice, CEMIP expression was negatively related to the abundance of active CD8$^+$ T cells (rho=−0.27, p=4.79e-09) but not central memory CD8$^+$ T cells in patients with CRC (rho=−0.047, p=0.316). Moreover, Gene Set Enrichment Analysis demonstrated that CEMIP was also strongly and negatively correlated with T-cell activation signaling in these patients (online supplemental figure 2C,D).

To validate whether tumor CEMIP directly affects CD8$^+$ T-cell antitumor activity, MC38-OVA cells expressing different levels of CEMIP were co-cultured with CD8$^+$ T cells isolated from the splenocytes of OT-I mice. CD8$^+$ T cells co-cultured with CEMIP^{KD} MC38 cells at a ratio of 5:1 or 10:1 showed higher proliferation and cytotoxic activities than those co-cultured with scramble MC38 cells (online supplemental figure 2E,F). Accordingly, CD8$^+$ T cells co-cultured with CEMIP^{KD} MC38 cells secreted strikingly higher levels of GZMB and IFN-γ (figure 1H,I). In addition, in order to determine the important role of CD8$^+$ T cells in regulating the growth of CEMIP-deficient tumors, we used the neutralizing anti-CD8 antibody to deplete CD8$^+$ T cells in vivo (online supplemental figure 3A). The result showed that depleting CD8$^+$ T cells abolished the growth delay of CEMIP^{KD} tumors (figure 1J and online supplemental figure 3B,C). Collectively, these results demonstrate that CEMIP drives tumor growth and inhibits the antitumor activity of CD8$^+$ T cells.

CEMIP downregulates MHC-I expression and impairs antigen presentation

We next examined how CEMIP prevents CD8$^+$ T-cell cytotoxicity. Considering the key role of MHC-I in CD8$^+$ T-cell activation,[27] we hypothesized that CEMIP might reduce the expression of MHC-I in tumor cells. Indeed, we found that cells expressing high levels of CEMIP had low expression of MHC-I (online supplemental figure 4A,B). Consistently, western blotting results showed that the protein level of MHC-I decreased in CEMIP^{OE} SW480 cells, while it increased in CEMIP^{KD} SW480 cells (figure 2A). The same results were further observed in MC38 murine cells (figure 2B). Intriguingly, there were no obvious alterations at the messenger RNA (mRNA) level (online supplemental figure 4C). Next, we further examined the MHC-I levels on the tumor cell surface by flow cytometry. As shown in figure 2C,D, MHC-I levels on the tumor cell surface were significantly upregulated in CEMIP^{KD} cells compared with the scramble-control group, while they were attenuated in CEMIP^{OE} cells (p<0.05). In contrast, CEMIP failed to affect MHC-II (data not shown) and programmed death ligand-1 (PD-L1) (online supplemental figure 4D) expression on the MC38 cell surface.

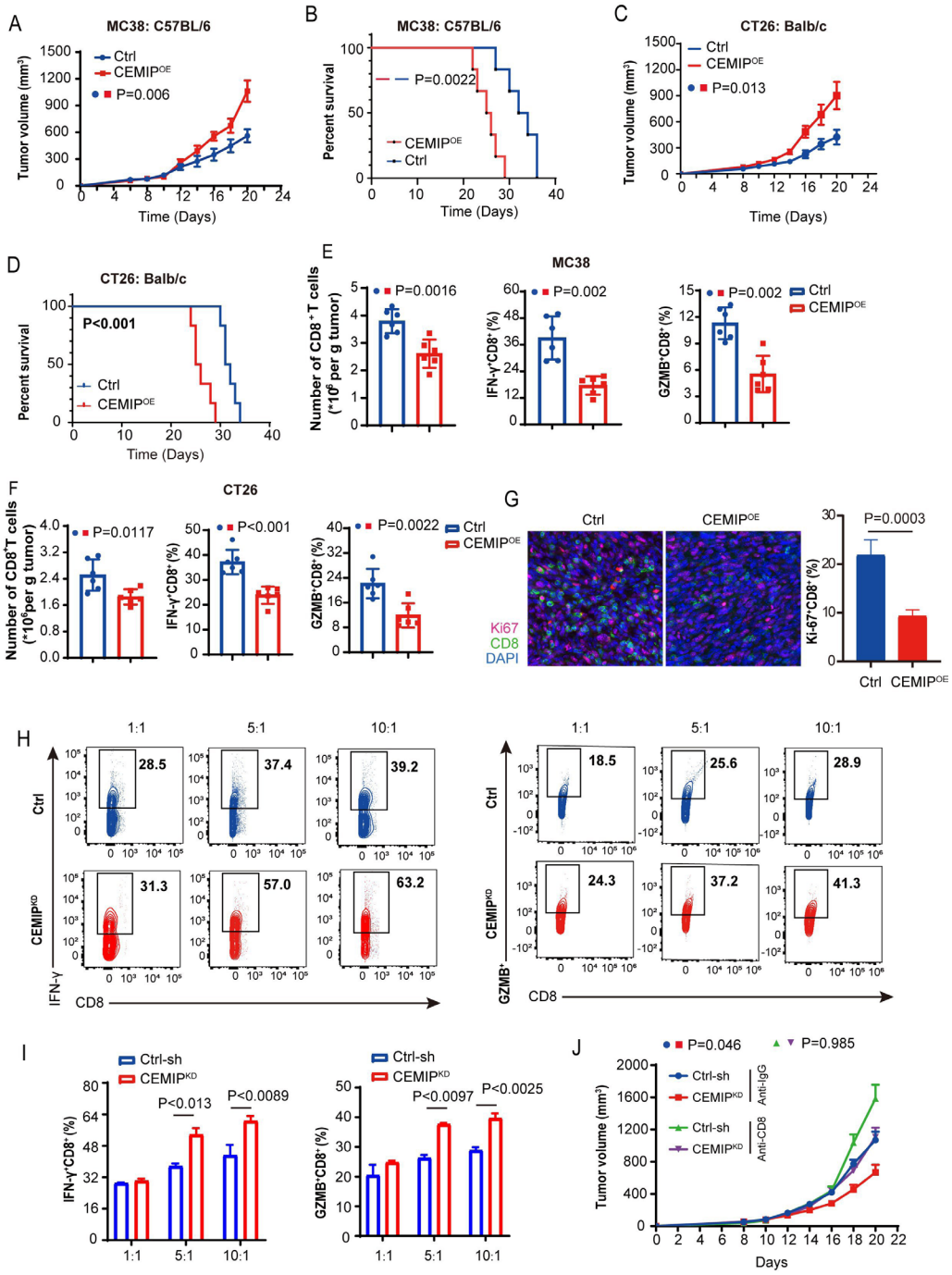

Figure 1 CEMIP promotes colon cancer cell growth in vivo and impacts the cytotoxicity of CD8$^+$ T cells. (A–B) Tumor growth volumes for C57BL/6 mice subcutaneously transplanted with 3×10^5 vector control (Ctrl) and CEMIP^{OE} MC38 cells. n=6 mice per group (A); Kaplan-Meier survival curves for these mice. n=8 mice/group, p values calculated by log-rank test (B). (C–D) Tumor growth volumes for Balb/c mice subcutaneously transplanted with 5×10^5 vector control (Ctrl) and CEMIP^{OE} CT26 cells. n=6 mice per group (C); Kaplan-Meier survival curves for these mice. n=8 mice per group, p values calculated by log-rank test (D). (E) Abundance of tumor-infiltrating CD8$^+$ T cells normalized by MC38 tumor weight per gram (left). The percentages of IFN-γ$^+$(middle) and GZMB$^+$ CD8$^+$(right) T cells in vector control and CEMIP^{OE} MC38 tumors were analyzed by flow cytometry. n=6/group. (F) Abundance of tumor-infiltrating CD8$^+$ T cells normalized by CT26 tumor weight per gram (left). The percentages of IFN-γ$^+$ (middle) and GZMB$^+$ CD8$^+$ (right) T cells in vector control and CEMIP^{OE} CT26 tumors were analyzed by flow cytometry. n=6/group. (G) Immunofluorescence staining (left) and quantitative estimates (right) of intratumoral Ki67-expressing CD8$^+$ T cells in vector control and CEMIP^{OE} MC38 tumors. Scale bar, 20 μm. n=3 independent samples. (H–I) MC38-ovalbumin cells with different CEMIP expression levels (Ctrl-sh or CEMIP^{KD}) were co-cultured with CD8$^+$ T cells isolated from the spleen of OT-I mice. After 72 hours, the activity of CD8$^+$ T cells was indicated by IFN-γ and GZMB levels. Representative flow cytometric data (H), and the quantitative results are summarized (I). n=3 biological replicates. All data are shown as the mean±SEM. (J) Tumor growth from control and CEMIP^{KD} MC38 tumor cells in C57BL/6 mice depleted of CD8$^+$ T cells. P value< 0.05 represents statistically significant. GZMB, granzyme B; IFN, interferon.

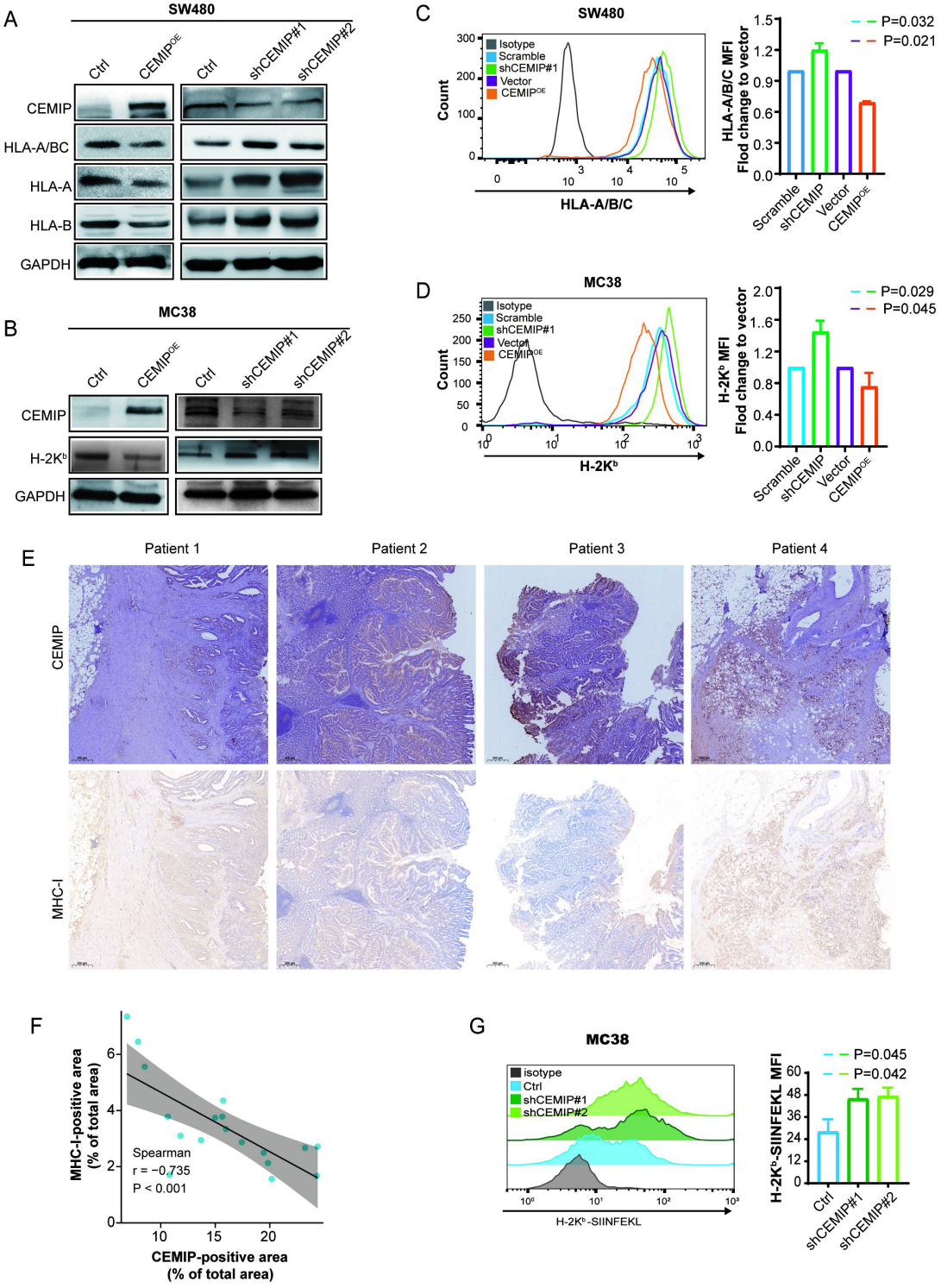

Figure 2 CEMIP downregulates the expression of MHC-I and impairs antigen presentation. (A) Overexpression or knockdown of CEMIP in SW480 cells and the expression of HLA-A/B/C, HLA-A, and HLA-B proteins were determined by western blotting analysis. (B) Overexpression or knockdown of CEMIP in MC38 cells and the expression of H-2K^b protein were determined by western blotting analysis. (C) Overexpression or knockdown of CEMIP in SW480 cells and flow cytometry-based quantification of plasma membrane levels of HLA-A/B/C. (D) Overexpression or knockdown of CEMIP in MC38 cells and flow cytometry-based quantification of plasma membrane levels of H-2K^b. (E) The expression of MHC-I and CEMIP from 19 patients with colorectal cancer was determined by immunohistochemistry. Representative images of four patients are shown. Scale bar, 500 µm. (F) The plot of the immunohistochemistry positive area of CEMIP versus that of MHC-I from patients (n=19 cases) was drawn, and Spearman's correlation coefficient along with the p value and 95% CI was shown. (G) Surface H-2K^{b}SIINFEKL was measured by flow cytometry in ovalbumin-expressing Ctrl or shCEMIP (#1 and #2) MC38 cells. n=3 biological replicates. All data are shown as the mean±SEM. P value<0.05 represents statistically significant. HLA, human leukocyte antigen MFI, mean fluorescent intensity; MHC-I, major histocompatibility complex class I.

Furthermore, immunohistochemistry and immunofluorescence staining revealed that CEMIP was negatively correlated with MHC-I expression in human CRC tumors, supporting our in vitro findings (figure 2E,F and online supplemental figure 4E). To evaluate antigen presentation, the neoantigen OVA was stably expressed in MC38 cells. As expected, we found increased surface expression of the OVA-derived peptide SIINFEKL bound to H-2K^b in CEMIP^{KD} OVA cells, confirming enhanced peptide presentation (figure 2G).

To assess whether CEMIP restricted CD8$^+$ T cell activities due to impaired MHC-I expression, we used an MHC-I blocking antibody in the co-culture of MC38-OVA or CT26-OVA and CD8$^+$ T cells. Notably, the MHC-I blocking antibody partially inhibited CD8$^+$ T proliferation and the expression of IFN-γ and GZMB in the setting of CEMIP^{KD} cells (figure 3A,B and online supplemental figure 5A,B). Next, MHC-I was blocked in vivo as described in a previous study.[15] In line with the in vitro results, MHC-I depletion in vivo rescued tumor growth and attenuated the percentage of tumor-infiltrating CD8$^+$ T cells and IFN-γ$^+$ CD8$^+$ T cells in CEMIP^{KD}cell-bearing mice (figure 3C–H). Overall, these data suggest that CEMIP impedes CD8$^+$ T-cell immunity by reducing MHC-I expression on tumor cells.

CEMIP promotes MHC-I internalization via clathrin-dependent endocytosis

How does CEMIP downregulate MHC-I expression on the tumor cell surface? A previous study reported that CEMIP facilitates the entry of hyaluronic acid into the cytoplasm for degradation through clathrin-dependent endocytosis.[28] Therefore, we asked whether CEMIP is involved in the endocytosis of MHC-I. As expected, the ratio of intracellular to plasma membrane MHC-I was significantly increased in CEMIP^{OE} cells compared with vector-control cells (figure 4A and online supplemental figure 6A), indicating that CEMIP could promote MHC-I endocytosis. The endocytosis of cells is mainly divided into clathrin-mediated and caveolae-mediated endocytosis, as well as other forms of endocytosis, including Arf6-dependent or cdc42-dependent endocytosis.[29–32] Next, we explored how CEMIP promoted MHC-I internalization. Flow cytometry was used to determine the level of MHC-I on the intracellular and plasma membranes after CEMIP^{OE} MC38 cells were treated with chlorpromazine (clathrin inhibitor), MβCD (caveolae inhibitor), NVA-2729 (ARF6 inhibitor), or ZCL278 (cdc42 inhibitor). Notably,the most pronounced inhibitory effect on MHC-I internalization was observed with the addition of chlorpromazine, suggesting that clathrin-dependent endocytosis might play a predominant role in CEMIP-mediated internalization of MHC-I (online supplemental figure 6B). In addition, when clathrin knockdown was executed in two murine cells by clathrin siRNA (online supplemental figure 6C), the levels of plasma membrane MHC-I substantially increased in CEMIP^{OE} cells but did not alter much in CEMIP^{KD} cells (figure 4B,C and online supplemental figure 6D). Furthermore, CEMIP-induced reduction of MHC-I levels on the cell surface were reversed by treatment with chlorpromazine in CEMIP^{OE} MC38-bearing mice. Meanwhile, chlorpromazine also delayed tumor growth and rescued the numbers of tumor-infiltrating CD8$^+$ T cells and IFN-γ$^+$ CD8$^+$ T cells (figure 4D–H). The same results were verified in CEMIP^{OE} CT26-bearing mice (figure 4I and online supplemental figure 6E–G). Overall, these results indicate that CEMIP plays an important role in regulating MHC-I internalization through clathrin-dependent endocytosis.

CEMIP promotes the interaction between MHC-I and clathrin

Generally, MHC-I internalization does not occur through clathrin-dependent endocytosis due to the lack of appropriate adaptors to link MHC-I and clathrin.[33] However, in our study, we found that MHC-I could be internalized via clathrin-dependent endocytosis in the presence of CEMIP. Therefore, we posited that CEMIP might act as an adaptor to promote the interaction between clathrin and MHC-I. Co-immunoprecipitation and proximity ligation assays revealed that CEMIP could directly coprecipitate with both endogenous clathrin and MHC-I (figure 5A–D). In particular, overexpression of CEMIP enhanced the interaction between endogenous clathrin and MHC-I (figure 5E,F). To further define which domain of CEMIP is involved in the interaction with clathrin and MHC-I, five truncated variants of CEMIP with a C-terminal MYC tag were established (online supplemental figure 6H). As shown in figure 5G–H, CEMIP-D (amino acids 820–1204) bound to MHC-I, and CEMIP-C (amino acids 572–819) interacted with clathrin. Taken together, CEMIP is a novel adaptor that facilitates the interaction between MHC-I and clathrin.

CEMIP anchors MHC-I to lysosomes for degradation

Similar to other cell surface receptors, MHC-I is destined to be recycled or degraded after internalization from the cell surface. The intracellular trafficking of MHC-I identified its co-localizationwith early endosomes, late endosomes, and lysosomes, as shown by immunofluorescence staining. We found that more MHC-I molecules were co-localized with late endosomes and lysosomes in both MC38- and SW480-CEMIP^{OE} cells (figure 6A and online supplemental figure 7A). Western blotting analysis confirmed that CEMIP increased H-2K^b expression in the lysosome fraction, while CEMIP knockdown elevated the H-2K^b level in the membrane fraction (figure 6B). Furthermore, when lysosome function was inhibited by treatment with bafilomycin, the total and plasma membrane MHC-I (H-2K^b) levels substantially increased in CEMIP^{OE} cells but did not change much in CEMIP^{KD} cells (figure 6C,D and online supplemental figure 7B). In accordance with the in vitro results, treatment of mice with the lysosomal inhibitor chloroquine after injection of CEMIP^{OE} CRC cells effectively delayed CEMIP-induced tumor growth, accompanied by restored MHC-I membrane expression and tumor-infiltrating CD8$^+$ T cells

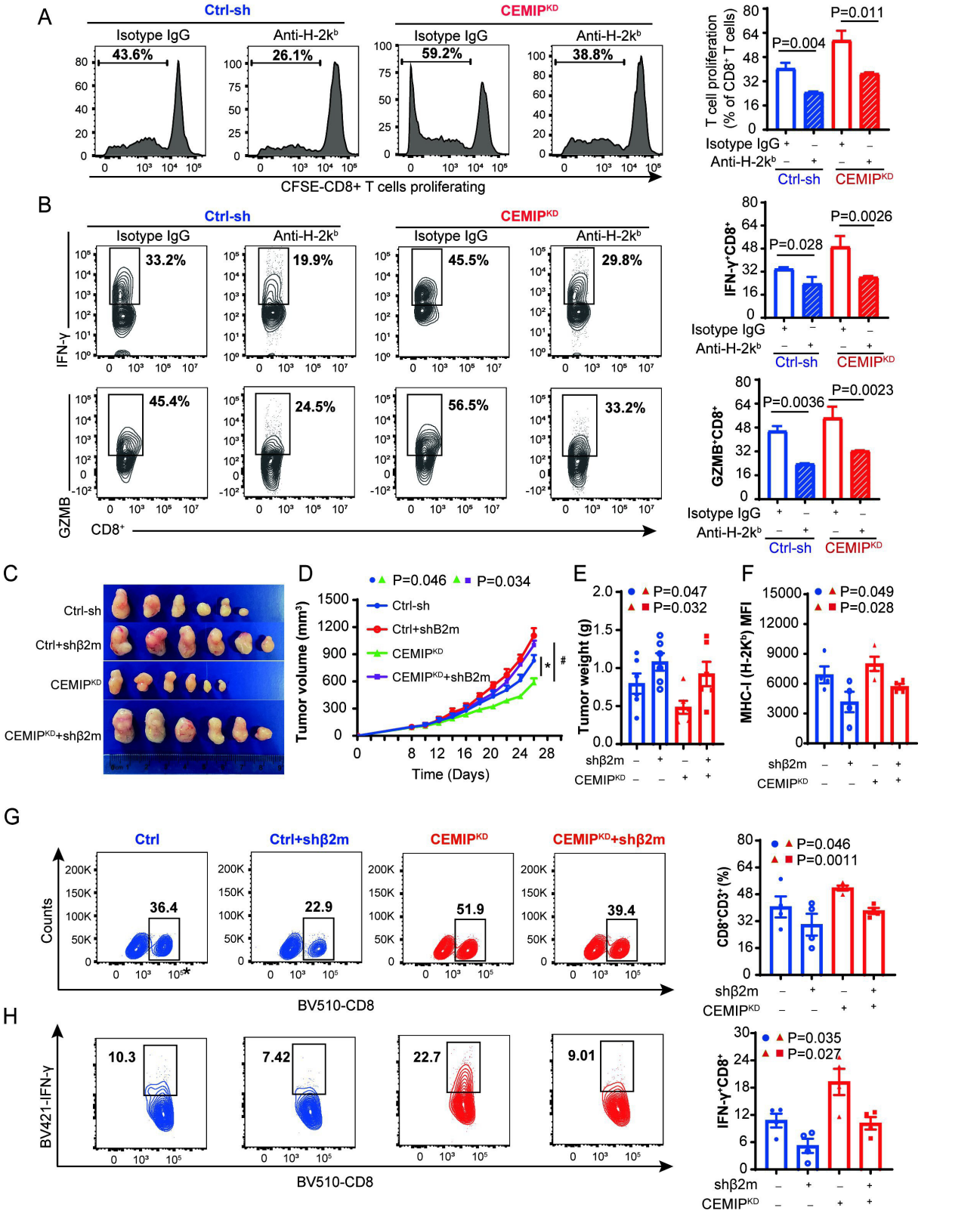

Figure 3 CEMIP restricted CD8$^+$ T-cell cytotoxicity partially due to impaired major histocompatibility complex class I expression. (A–B) MC38-ovalbumin cells were co-cultured with OT-I T cells with control isotype or H-2K^b blocking antibody. CD8$^+$ T-cell proliferation was measured by CFSE dilution (A), and the secretion of the cytokines granzyme B and IFN-γ by CD8$^+$ T cells was analyzed by flow cytometry (B). n=3 biological replicates. (C–E) C57BL/6 mice were subcutaneously injected with 3×10^5 Ctrl-sh and CEMIP^{KD} MC38 cells expressing shRNA against β2 m. Tumor image (C), volume (D), and weight (E) are shown. n=6 mice per group. (F–H) The level of H-2K^b (F) and the percentages of tumor-infiltrating CD8$^+$ T (G) and IFN-γ$^+$ CD8$^+$ T cells (H) in the MC38 tumors were analyzed by flow cytometry. All data are shown as the mean±SEM. n=4/group. P value<0.05 represents statistically significant. CFSE, carboxyfluorescein diacetate succinimide ester; IFN, interferon; GZMB, granzyme B.

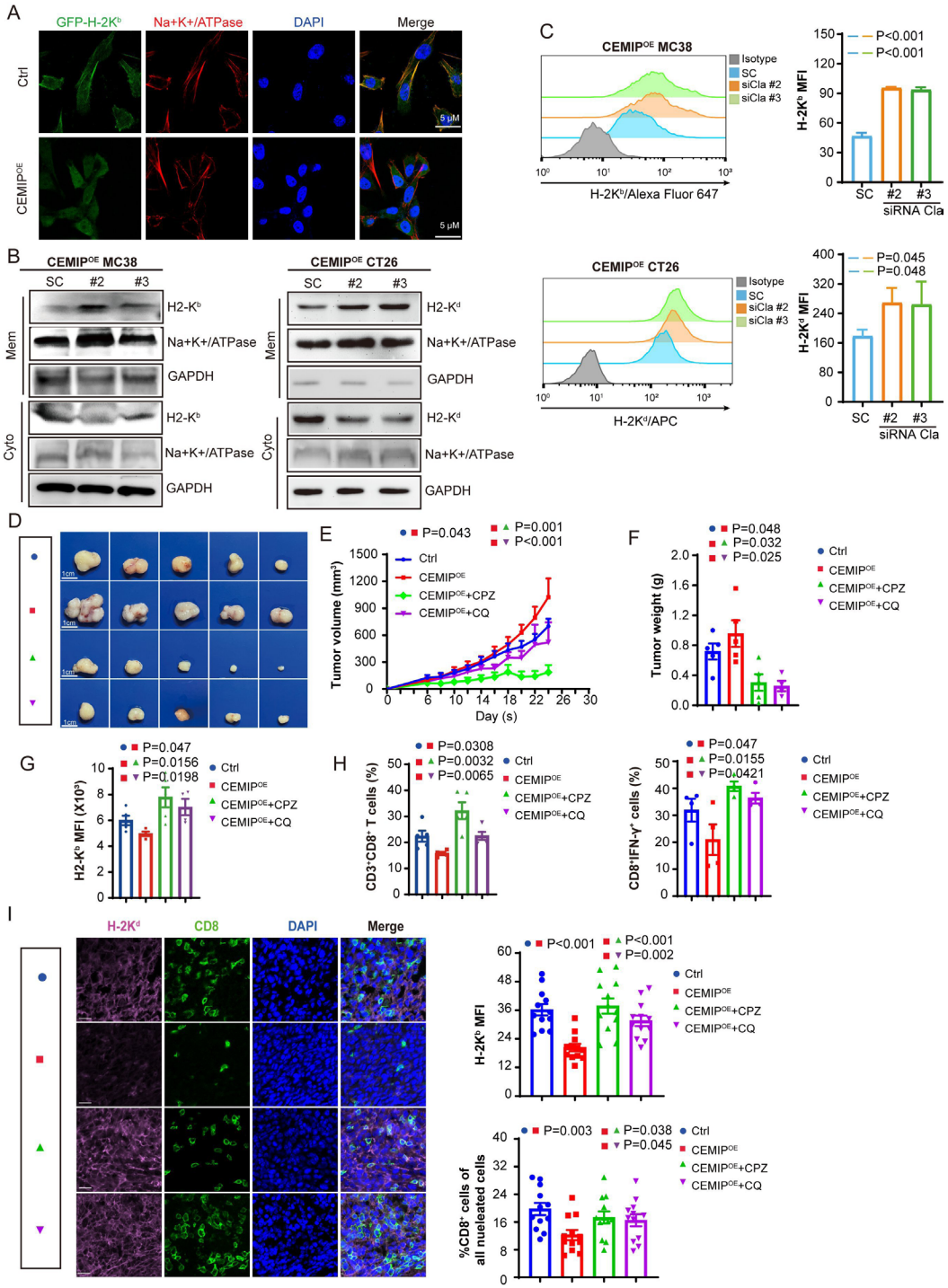

Figure 4 CEMIP promotes MHC-I internalization via clathrin-mediated endocytosis. (A) The expression of H-2Kb (green) in the cytosolic and plasma membrane fractions of CEMIP^{OE} and Ctrl MC38 cells was detected by immunofluorescence. Na+K+/ATPase (red) was used to stain cell membrane. n=3 independent experiments; Scale bars, 5 μm. (B) Western blotting quantification of MHC-I in the cytosolic and plasma membrane fractions of CEMIP^{OE} MC38 (H-2K^{b}, left) and CT26 (H-2K^{d}, right) cells transfected with siRNA clathrin (siCla) or control siRNA (SC), respectively. (C) Surface H-2K^{b} was measured by flow cytometry in CEMIP^{OE} MC38 and CEMIP^{OE} CT26 cells transfected with siRNA clathrin (siCla) or control siRNA (SC), respectively. (D–F) Tumor growth was monitored in C57/BL6 mice bearing Ctrl and CEMIP^{OE} MC38 cells treated with the clathrin inhibitor chlorpromazine or the lysosome inhibitor chloroquine. Tumor image (D), volume (E), and weight (F) are shown. n=5/group. Scale bars,1 cm. (G–H) Tumors from the above mice were collected. The level of H-2K^{b} (G) and the percentages of tumor-infiltrating CD8^{+} and interferon-γ^{+} CD8^{+} T cells (H) were analyzed by flow cytometry. n=4/group. (I) CEMIP^{OE} and Ctrl CT26 cells were inoculated into BALB/c mice. The levels of H-2K^{d} (pink) and tumor-infiltrating CD8^{+} T cells (green) were analyzed by immunofluorescence. Scale bar, 20 μm. n=3 independent samples; four fluorescent fields of each sample were counted by ImageJ. All data are shown as the mean±SEM. P value< 0.05 represents statistically significant. MFI, mean fluorescent intensity; MHC-I, major histocompatibility complex class I.

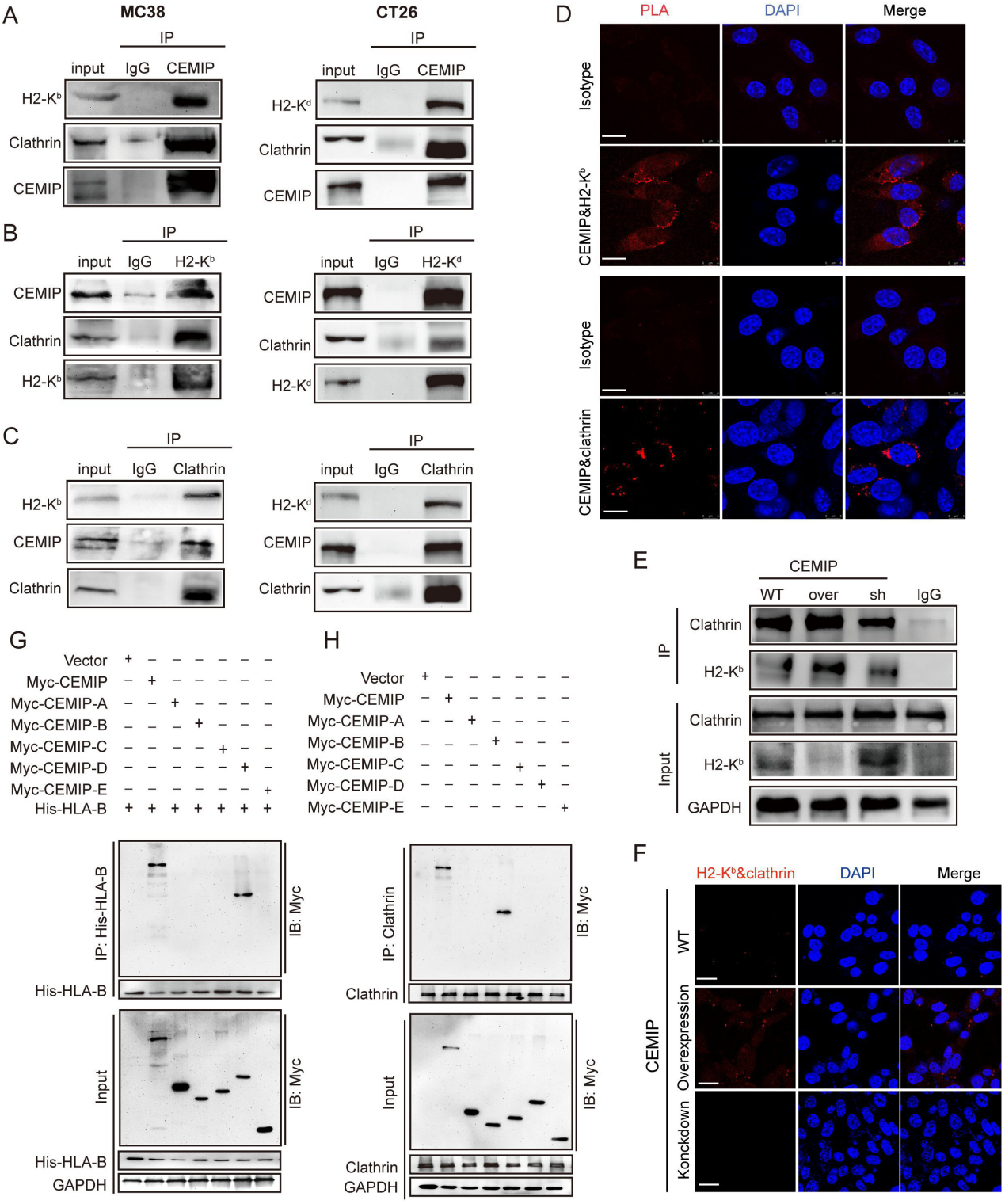

Figure 5 CEMIP promotes the interaction of MHC-I and clathrin. (A–C) Co-IP analysis of the interaction between CEMIP and MHC-I or clathrin. Whole-cell extracts from MC38 or CT26 cells were immunoprecipitated with the indicated antibodies. (D) Duolink in situ PLA was adopted for detecting the interaction between CEMIP and MHC-I (H-2K^b) or clathrin in MC38 cells. Anti-CEMIP, anti-H-2K^b, or anti-clathrin were used as primary antibodies. IgG was used as a staining control. Scale bar, 20 µm. (E) CEMIP mediates the interaction of MHC-I (H-2K^b) and clathrin. MC38 cells with different CEMIP expression levels were lysed. Endogenous clathrin-antibody was immunoprecipitated for western blotting analysis. (F) CEMIP regulates the interaction of MHC-I (H-2K^b) and clathrin in MC38 cells. A proximity ligation assay was applied. Red: co-localized MHC-I (H-2K^b) and clathrin in situ; blue, DAPI for nuclear staining. Scale bar, 20 µm. (G–H) Western blotting analysis of proteins derived from Co-IP in 293 T cells transduced with plasmids as indicated. CEMIP-D (aa 820–1204) binds to MHC-I, and CEMIP-C (aa 572–819) binds to clathrin. Co-IP, Co-Immunoprecipitation; DAPI, 4',6-diamidino-2-phenylindole; PLA, Proximity Ligation Assay; HLA, human leukocyte antigen; MHC-I, major histocompatibility complex class I; WT, wild type.

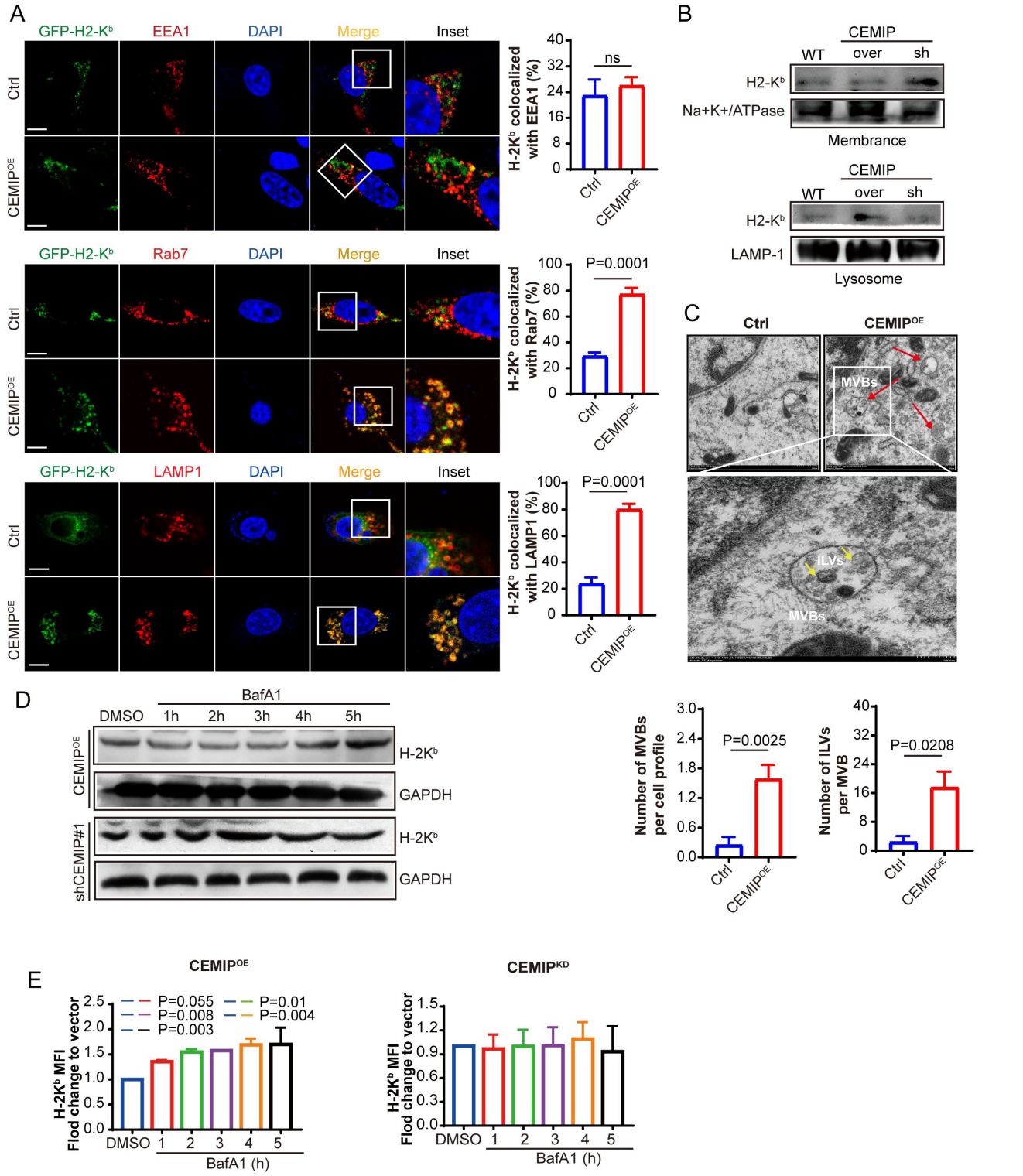

Figure 6 CEMIP anchors MHC-I to lysosomes for degradation. (A) Confocal micrographs of Ctrl and CEMIP^{OE} MC38 cells stained for H-2K^b and EEA1, Rab7, or LAMP1 markers. Scale bar, 20 µm. Bar graphs depict % colocalization shown for the respective markers in boxed insets (Manders' coefficient). (B) Western blotting quantification of MHC-I (H-2K^b) in the plasma membrane (top) and lysosome (bottom) fractions of wild type (WT), CEMIP^{OE}, and CEMIP^{KD} MC38 cells. (C) Representative electron microscopic images of Ctrl and CEMIP^{OE} MC38 cells. Scale bar, 1 µm. Zooms (lower panels) are ×4.8. Red arrows indicate MVBs containing typical intraluminal vesicles (ILVs) (yellow arrows). The number of MVBs per cell profile and the number of ILVs per MVB were counted in eight profiles of different cells. (D) Western blotting analysis of MHC-I (H-2K^b) expression in CEMIP^{OE} and CEMIP^{KD} MC38 cells treated with 150 nM bafilomycin A1 (BafA1) for the indicated time. (E) Surface MHC-I (H-2K^b) levels were measured by flow cytometry in CEMIP^{OE} and CEMIP^{KD} MC38 cells treated with 150 nM bafilomycin A1 (BafA1) for the indicated time. All data are shown as the mean±SEM. P value<0.05 represents statistically significant. MFI, mean fluorescent intensity; MHC-I, major histocompatibility complex class I; MVBs, multivesicular bodies; ns, not significant.

(figure 4D–I). Lysosome-mediated degradation requires the formation of multivesicular bodies (MVBs).[34] Electron microscopy analysis revealed the role of CEMIP in promoting MVB formation, as the numbers of MVBs and intraluminal vesicles were higher in CEMIP^{OE} cells (figure 6E). Protein ubiquitination is often implicated in MVB processes.[35] As shown in online supplemental figure 7C,thedecreased ubiquitylation of MHC-I was obviously present in CEMIP^{KD} cells. Collectively, these data suggest that CEMIP downregulates MHC-I levels by lysosome-mediated degradation.

CEMIP inhibition sensitizes CRC to ICB

MHC-I deficiency impairs CD8$^+$ T-cell recognition and activation as a major ICB resistance mechanism.[36] Given that CEMIP could suppress the antitumor immunity of CD8$^+$ T cells by reducing MHC-I levels on the cell surface, we sought to determine whether CEMIP inhibition could synergize with ICB therapy. First, we treated established syngeneic mice bearing scramble control or CEMIP^{KD} MC38 cells with dual ICB (anti-PD-1 and anti-CTLA-4 antibodies) on day 3 after tumor cell inoculation (figure 7A). We observed moderately reduced tumor growth in mice treated with ICB therapy alone or inoculated with CEMIP^{KD} alone (figure 7B,C). More importantly, CEMIP inhibition in combination with ICB further attenuated tumor growth compared with CEMIP^{KD} alone or ICB alone. Furthermore, tumors treated with CEMIP inhibition plus ICB exhibited increased infiltration of

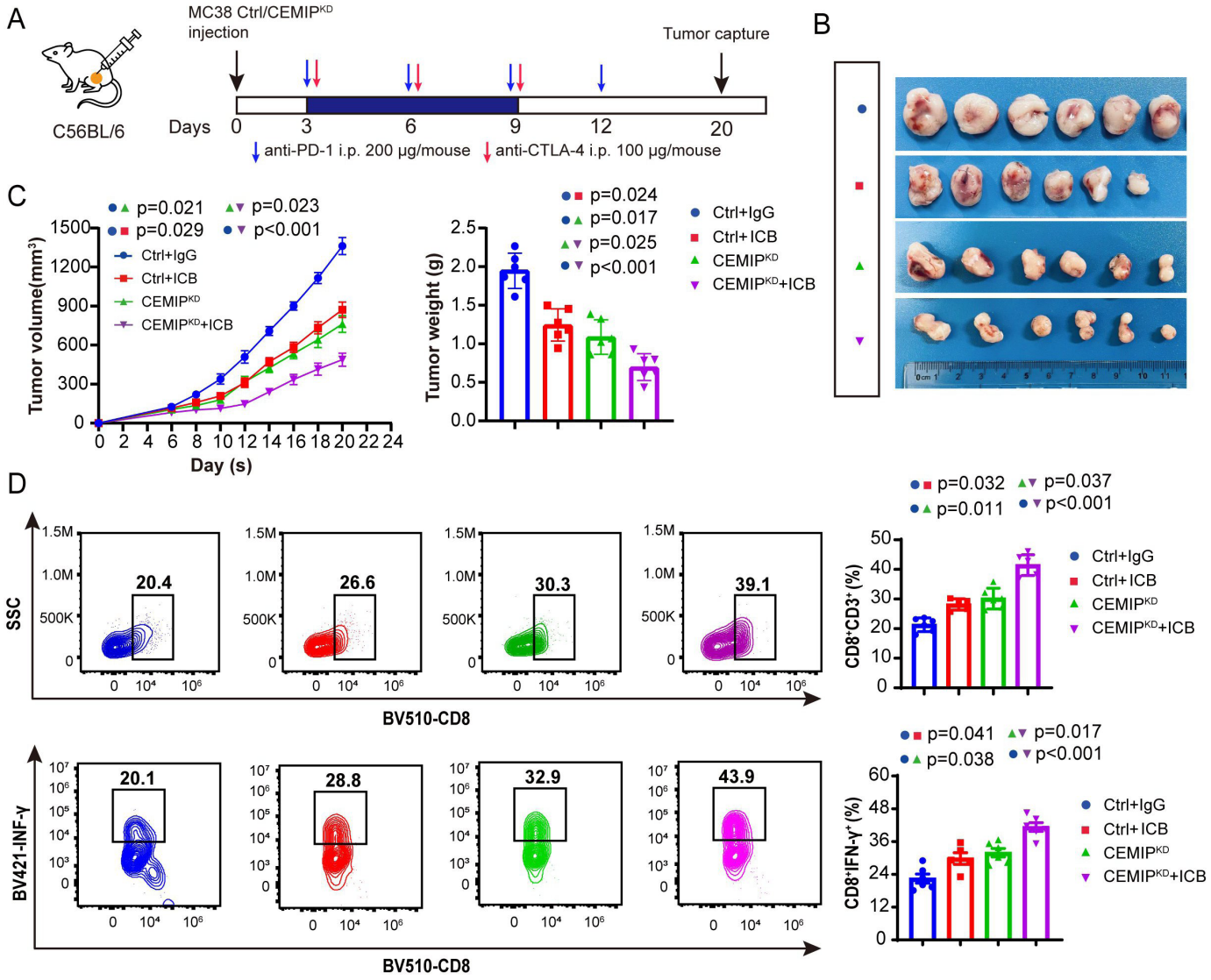

Figure 7 CEMIP inhibition increases the sensitivity of colon cancer cells to immune checkpoint blockade. (A–C) C57BL/6 mice were implanted with 3×10^5 Ctrl or CEMIP^{KD} cells and received PD-1 mAb treatment plus CTLA-4 mAb or IgG isotype control (IgG). A schematic view of the treatment plan (A), tumor image (B), tumor volume, and weight (C) were measured every 2 days. n=6 mice per group. (D) Tumors from the above mice were collected. The percentages of tumor-infiltrating CD8$^+$ and IFN-γ$^+$ CD8$^+$ T cells were analyzed by flow cytometry. n=5–6/group. All data are shown as the mean±SEM. P value<0.05 represents statistically significant. mAb, monoclonal antibodie; SSC,side scatter; CTLA-4, cytotoxic T-lymphocytes-associated protein 4; ICB, immune checkpoint blockade; IFN, interferon; PD-1, programmed cell death protein-1.

$CD8^+$ T cells and IFN-γ^+CD8^+ T cells compared with the $CEMIP^{KD}$ group (figure 7D). Second, we also performed an additional mouse experiment where mice were intraperitoneally injected with dual ICB on day 8 when the tumor volumes were larger (online supplemental figure 8C). Consistent with the above results, the combination of CEMIP inhibition and ICB was superior in terms of tumor growth reduction compared with CEMIP inhibition alone (online supplemental figure 8B,C). Meanwhile, the number of tumor-infiltrating $CD8^+$ T cells, as well as the percentage of IFN-γ^+or $GZMB^+$ $CD8^+$ T cells, was highest in the group treated with a combination of CEMIP inhibition and ICB (online supplemental figure 8E). Moreover, the expression of CTLA-4 and PD-1 by the intratumoral $CD8^+$ T cells was significantly lower in $CEMIP^{KD}$+ICB group than in the other groups (online supplemental figure 8F). These results indicate that CEMIP inhibition sensitizes CRC tumors to ICB therapy.

Current data has shown that patients with CRC with MSI-H are more sensitive to ICB therapy compared with patients with CRC with microsatellite stability (MSS)/microsatellite instability-low (MSI-L). MSI-H has been demonstrated to be a reliable predictor for ICB efficacy. To explore the correlation between CEMIP and MSI/MSS in CRC, we used The Cancer Genome Atlas database to analyze the expression of CEMIP in patients with CRC with MSS/MSI-L and MSI-H. The results showed that the expression of CEMIP in MSI-H patients was significantly lower than that in MSS/MSI-L patients (online supplemental figure 8G). This was in line with the results in mice, where the expression of CEMIP was negatively correlated with the sensitivity of ICB therapy, suggesting that the level of CEMIP in tumor tissue may be a biomarker to predict the efficacy of immunotherapy.

DISCUSSION

The dramatic successes of ICB therapy do not provide therapeutic benefits to the majority of patients with CRC. Here, we identify tumor cell-intrinsic CEMIP as a key player that contributes to immune evasion in CRC. In this work, we demonstrate that CEMIP promotes immune evasion of colon cancer cells by impairing MHC-I antigen presentation, resulting in the inhibition of $CD8^+$ T-cell antitumor activity. CEMIP inhibition enhances the efficacy of ICB therapy for CRC. Mechanistically, CEMIP is an adaptor that facilitates the interaction between MHC-I and clathrin, which drives MHC-I internalization via clathrin-mediated endocytosis and subsequent sequestration within the lysosome for degradation. Collectively, our study reveals a novel regulatory mechanism of MHC-I on the tumor surface and provides a novel treatment strategy for CRC immunotherapy.

We previously reported that high expression of CEMIP in tumor tissues was a biomarker of poor prognosis in patients with CRC.[25 37 38] One top hit, CEMIP failed to mediate CRC cell proliferation in vitro or in immunodeficient mice,[26] yet it drove tumor growth in immunocompetent mice mainly by preventing $CD8^+$ T-cell cytotoxicity in our study. This is in line with a recent study showing that CEMIP is strongly correlated with reduced infiltration of $CD8^+$ T cells in liver metastasis.[37] Together, these results suggest that CEMIP is a critical suppressor gene in the regulation of the immune response, which can help cancer cells evade immune attacks. MHC-I-mediated antigen presentation by cancer cells constitutes a central focus of antitumor $CD8^+$ T-cell responses. A growing body of evidence suggests that enhancing MHC-I levels in cancer cells could increase the $CD8^+$ T-cell immune response and improve ICB efficacy.[14 36 39] However, upregulation of MHC-I may also be accompanied by increased PD-L1, with opposite effects on tumor immunity.[36] In the present study, we proved that CEMIP reduced the expression of MHC-I on the tumor cell surface without any effect on PD-L1, suggesting that CEMIP is a specific MHC-I negative regulator. Blocking MHC-I inhibited $CD8^+$ T-cell antitumor immunity in the setting of $CEMIP^{KD}$ cells. These results demonstrate that CEMIP is a prospective target for patients with CRC resistant to immunotherapy. Accordingly, targeted inhibition of CEMIP synergistically enhanced the efficacy of ICB therapy for CRC tumors. These findings raise the unexplored possibility of CEMIP-based therapy, either in the form of inhibitors or monoclonal CEMIP antibodies, in the future.

MHC-I downregulation in cancer is driven by several mechanisms, including genetic defects, transcriptional silencing via various transcription factors (nuclear factor-kB, multiple IFN regulatory factors, and NLRC5), and epigenetic regulation through DNA hypermethylation and histone deacetylation.[40–42] In this study, we revealed that CEMIP could downregulate the expression of MHC-I at the protein level rather than the mRNA level. Recently, a published study showed that MHC-I is selectively targeted for lysosomal degradation via an autophagy-dependent mechanism in pancreatic cancer, leading to reduced expression of MHC-I on the cell surface.[15] Moreover, other studies demonstrate that excessive internalization of MHC-I driven by the oncogenes MAL2 or $BRAF^{V600E}$ also decreases MHC-I levels on the cell surface and induces immune escape.[43 44] These findings highlight concerns about how MHC-I trafficking mechanisms can be associated with tumor immune escape. Our data expand on these modes of regulation in CRC. We revealed that CEMIP could drive MHC-I internalization via clathrin-mediated endocytosis and then anchor MHC-I to lysosomes for degradation. Blocking clathrin or lysosomes with inhibitors could support cancer immunotherapy and inhibit tumor growth by upregulating the expression of MHC-I on the tumor cell surface. Notably, MHC-I internalization is generally thought not to occur through clathrin-dependent endocytosis due to the lack of appropriate adaptors.[33] The function of adaptors is to bridge cargo and clathrin, a critical step in clathrin-dependent endocytosis.[30] Here, we identified CEMIP as a new adaptor that bridges clathrin with MHC-I to drive

MHC-I internalization via clathrin-mediated endocytosis. Notably, the domains of CEMIP that interacted with clathrin and MHC-I were different. MHC-I is bound to the domain amino acids 820–1204, while clathrin interacts with the domain amino acids 572–819. Other domains of CEMIP were not involved in this function. Previous literature shows that CEMIP is located in clathrin-coated vesicles and binds with clathrin, which reinforces our results.[28] Our study refines the mechanism of MHC-I internalization.

CEMIP is not only associated with a poor prognosis in CRC but also correlates with the progression of other human malignancies, such as breast cancer, gastric cancer, and pancreatic cancer.[45 46] It will make sense to determine to what extent other tumors use CEMIP misdirection of MHC-I for immune evasion. If validated, these findings will expand the evidence that targeting CEMIP is a good choice for improving ICB efficacy in tumors with MHC-I deficiency. Moreover, dMMR/MSI-H is currently a clear biomarker of potential response to immunotherapy for colorectal tumors,[47] but the high mutational burden alone does not seem to be sufficient for driving immunotherapy response.[48] The presence of tumor-infiltrating $CD8^+$ T cells is a prognostic factor for clinical outcomes in patient with CRC.[49 50] CEMIP was found to be an important suppressor of $CD8^+$ T-cell infiltration and activity in CRC, suggesting that CEMIP levels maybe included in the biomarker panel for ICB therapy. Further studies need to be performed.

Conclusion

In summary, this study demonstrates that CEMIP plays a key role in immune escape by downregulating MHC I levels on the cell surface. Moreover, we reveal that CEMIP is an adaptor that facilitates the interaction between MHC-I and clathrin, which drives MHC-I internalization via clathrin-mediated endocytosis and then promotes its degradation in lysosomes. Thus, our study elucidates a novel molecular mechanism of MHC-I downregulation. In addition, CEMIP inhibition is potentially an effective strategy for cancer immunotherapy.

Acknowledgements We acknowledge support from the National Natural Science Foundation of China (81874061, 81874084, and 82072800). We thank Weihong Chen for the technical support of the project.

Contributors BZ, JR, JL and TZ contributed to the conception or design of the work. BZ, JR, QH, JL, HW, GX, YZ and ZL contributed to the acquisition, analysis, or interpretation of the data. LW, JC, RL. MJ, JT. LZ, DZ, DY and QL provided advice and technical assistance. BZ and JL drafted the work, and all authors revised the draft. Guarantors: TZ.

Funding This study was supported by a grant from the National Natural Science Foundation of China (82203013, 81874061, 81874084, 82072800).

Competing interests None declared.

Patient consent for publication Not applicable.

Ethics approval All animal experiments were approved by The Medical Ethics Committee of Tongji Medical College, Huazhong University of Science and Technology, and performed according to the National Institutes of Health animal use guidelines on the use of experimental animals.

Provenance and peer review Not commissioned; externally peer reviewed.

Data availability statement All data relevant to the study are included in the article or uploaded as supplementary information.

ORCID iD

Tao Zhang http://orcid.org/0000-0003-4018-3393

REFERENCES

1 Topalian SL, Drake CG, Pardoll DM. Immune checkpoint blockade: a common denominator approach to cancer therapy. *Cancer Cell* 2015;27:450–61.
2 Ribas A, Wolchok JD. Cancer immunotherapy using checkpoint blockade. *Science* 2018;359:1350–5.
3 Chen L, Han X. Anti-PD-1/PD-L1 therapy of human cancer: past, present, and future. *J Clin Invest* 2015;125:3384–91.
4 Sharma P, Hu-Lieskovan S, Wargo JA, *et al*. Primary, adaptive, and acquired resistance to cancer immunotherapy. *Cell* 2017;168:707–23.
5 Yewdell JW, Dersh D, Fåhraeus R. Peptide channeling: the key to MHC class I immunosurveillance? *Trends Cell Biol* 2019;29:929–39.
6 Jhunjhunwala S, Hammer C, Delamarre L. Antigen presentation in cancer: insights into tumour immunogenicity and immune evasion. *Nat Rev Cancer* 2021;21:298–312.
7 Wang S, He Z, Wang X, *et al*. Antigen presentation and tumor immunogenicity in cancer immunotherapy response prediction. *Elife* 2019;8:49020. doi:10.7554/eLife.49020
8 McGranahan N, Rosenthal R, Hiley CT, *et al*. Allele-specific HLA loss and immune escape in lung cancer evolution. *Cell* 2017;171:1259–71.
9 Vitale M, Rezzani R, Rodella L, *et al*. HLA class I antigen and transporter associated with antigen processing (TAP1 and TAP2) down-regulation in high-grade primary breast carcinoma lesions. *Cancer Res* 1998;58:737–42.
10 Krishnakumar S, Abhyankar D, Sundaram AL, *et al*. Major histocompatibility antigens and antigen-processing molecules in uveal melanoma. *Clin Cancer Res* 2003;9:4159–64.
11 Simpson JAD, Al-Attar A, Watson NFS, *et al*. Intratumoral T cell infiltration, MHC class I and STAT1 as biomarkers of good prognosis in colorectal cancer. *Gut* 2010;59:926–33.
12 Raskov H, Orhan A, Christensen JP, *et al*. Cytotoxic $CD8^+$ T cells in cancer and cancer immunotherapy. *Br J Cancer* 2021;124:359–67.
13 Cornel AM, Mimpen IL, Nierkens S. MHC class I downregulation in cancer: underlying mechanisms and potential targets for cancer immunotherapy. *Cancers* 2020;12:12071760. doi:10.3390/cancers12071760
14 Taylor BC, Balko JM. Mechanisms of MHC-I downregulation and role in immunotherapy response. *Front Immunol* 2022;13:844866.
15 Yamamoto K, Venida A, Yano J, *et al*. Autophagy promotes immune evasion of pancreatic cancer by degrading MHC-I. *Nature* 2020;581:100–5.
16 Liu X, Bao X, Hu M, *et al*. Inhibition of PCSK9 potentiates immune checkpoint therapy for cancer. *Nature* 2020;588:693–8.
17 Dersh D, Yewdell JW. Immune MAL2-practice: breast cancer immunoevasion via MHC class I degradation. *J Clin Invest* 2021;131:144344. doi:10.1172/JCI144344
18 Montealegre S, van Endert PM. Endocytic recycling of MHC class I molecules in non-professional antigen presenting and dendritic cells. *Front Immunol* 2018;9:3098.
19 Naslavsky N, Caplan S. The enigmatic endosome - sorting the ins and outs of endocytic trafficking. *J Cell Sci* 2018;131:216499. doi:10.1242/jcs.216499

20 van Endert P. Intracellular recycling and cross-presentation by MHC class I molecules. *Immunol Rev* 2016;272:80–96.
21 Sung H, Ferlay J, Siegel RL, *et al*. Global cancer statistics 2020: GLOBOCAN estimates of incidence and mortality worldwide for 36 cancers in 185 countries. *CA Cancer J Clin* 2021;71:209–49.
22 André T, Shiu K-K, Kim TW, *et al*. Pembrolizumab in microsatellite-instability-high advanced colorectal cancer. *N Engl J Med* 2020;383:2207–18.
23 Sade-Feldman M, Jiao YJ, Chen JH, *et al*. Resistance to checkpoint blockade therapy through inactivation of antigen presentation. *Nat Commun* 2017;8:1136.
24 Rooney MS, Shukla SA, Wu CJ, *et al*. Molecular and genetic properties of tumors associated with local immune cytolytic activity. *Cell* 2015;160:48–61.
25 Zhang D, Zhao L, Shen Q, *et al*. Down-regulation of KIAA1199/CEMIP by miR-216a suppresses tumor invasion and metastasis in colorectal cancer. *Int J Cancer* 2017;140:2298–309.
26 Zhao L, Zhang D, Shen Q, *et al*. KIAA1199 promotes metastasis of colorectal cancer cells via microtubule destabilization regulated by a PP2A/stathmin pathway. *Oncogene* 2019;38:935–49.
27 Wieczorek M, Abualrous ET, Sticht J, *et al*. Major histocompatibility complex (MHC) class I and MHC class II proteins: conformational plasticity in antigen presentation. *Front Immunol* 2017;8:292.
28 Yoshida H, Nagaoka A, Kusaka-Kikushima A, *et al*. KIAA1199, a deafness gene of unknown function, is a new hyaluronan binding protein involved in hyaluronan depolymerization. *Proc Natl Acad Sci U S A* 2013;110:5612–7.
29 El-Sayed A, Harashima H. Endocytosis of gene delivery vectors: from clathrin-dependent to lipid raft-mediated endocytosis. *Mol Ther* 2013;21:1118–30.
30 Kaksonen M, Roux A. Mechanisms of clathrin-mediated endocytosis. *Nat Rev Mol Cell Biol* 2018;19:313–26.
31 Nabi IR, Le PU. Caveolae/raft-dependent endocytosis. *J Cell Biol* 2003;161:673–7.
32 Schweitzer JK, Sedgwick AE, D'Souza-Schorey C. ARF6-mediated endocytic recycling impacts cell movement, cell division and lipid homeostasis. *Semin Cell Dev Biol* 2011;22:39–47.
33 Adiko AC, Babdor J, Gutiérrez-Martínez E, *et al*. Intracellular transport routes for MHC I and their relevance for antigen cross-presentation. *Front Immunol* 2015;6:335.
34 Piper RC, Katzmann DJ. Biogenesis and function of multivesicular bodies. *Annu Rev Cell Dev Biol* 2007;23:519–47.
35 Katzmann DJ, Babst M, Emr SD. Ubiquitin-dependent sorting into the multivesicular body pathway requires the function of a conserved endosomal protein sorting complex, ESCRT-I. *Cell* 2001;106:145–55.
36 Gu SS, Zhang W, Wang X, *et al*. Therapeutically increasing MHC-I expression potentiates immune checkpoint blockade. *Cancer Discov* 2021;11:1524–41.
37 Wang H, Zhang B, Li R, *et al*. KIAA1199 drives immune suppression to promote colorectal cancer liver metastasis by modulating neutrophil infiltration. *Hepatology* 2022;76:967–81.
38 Hua Q, Zhang B, Xu G, *et al*. CEMIP, a novel adaptor protein of OGT, promotes colorectal cancer metastasis through glutamine metabolic reprogramming via reciprocal regulation of β-catenin. *Oncogene* 2021;40:6443–55.
39 Gettinger S, Choi J, Hastings K, *et al*. Impaired HLA class I antigen processing and presentation as a mechanism of acquired resistance to immune checkpoint inhibitors in lung cancer. *Cancer Discov* 2017;7:1420–35.
40 van den Elsen PJ, Holling TM, Kuipers HF, *et al*. Transcriptional regulation of antigen presentation. *Curr Opin Immunol* 2004;16:67–75.
41 Jongsma MLM, Guarda G, Spaapen RM. The regulatory network behind MHC class I expression. *Mol Immunol* 2019;113:16–21.
42 Zhou Y, Bastian IN, Long MD, *et al*. Activation of NF-κB and p300/CBP potentiates cancer chemoimmunotherapy through induction of MHC-I antigen presentation. *Proc Natl Acad Sci U S A* 2021;118:2025840118. doi:10.1073/pnas.2025840118
43 Fang Y, Wang L, Wan C. MAL2 drives immune evasion in breast cancer by suppressing tumor antigen presentation. *J Clin Invest* 2020.
44 Bradley SD, Chen Z, Melendez B, *et al*. BRAFV600E co-opts a conserved MHC class I internalization pathway to diminish antigen presentation and CD8+ T-cell recognition of melanoma. *Cancer Immunol Res* 2015;3:602–9.
45 Jami M-S, Hou J, Liu M, *et al*. Functional proteomic analysis reveals the involvement of KIAA1199 in breast cancer growth, motility and invasiveness. *BMC Cancer* 2014;14:194.
46 Koga A, Sato N, Kohi S, *et al*. KIAA1199/CEMIP/HYBID overexpression predicts poor prognosis in pancreatic ductal adenocarcinoma. *Pancreatology* 2017;17:115–22.
47 Ganesh K, Stadler ZK, Cercek A, *et al*. Immunotherapy in colorectal cancer: rationale, challenges and potential. *Nat Rev Gastroenterol Hepatol* 2019;16:361–75.
48 Chan TA, Yarchoan M, Jaffee E, *et al*. Development of tumor mutation burden as an immunotherapy biomarker: utility for the oncology clinic. *Ann Oncol* 2019;30:44–56.
49 Reissfelder C, Stamova S, Gossmann C, *et al*. Tumor-specific cytotoxic T lymphocyte activity determines colorectal cancer patient prognosis. *J Clin Invest* 2015;125:739–51.
50 Pagès F, Mlecnik B, Marliot F, *et al*. International validation of the consensus immunoscore for the classification of colon cancer: a prognostic and accuracy study. *Lancet* 2018;391:2128–39.